Journal of Forestry Research (2026) 37:90
https://doi.org/10.1007/s11676-026-02033-y

ORIGINAL PAPER

Biomass response of *Schinus terebinthifolia* to elevated ozone: evidence for a dose-dependent hormetic effect

Matheus Casarini Siqueira[1,2] · Barbara Baesso Moura[3,4] · Yasutomo Hoshika[3,4] · Elena Paoletti[3,4] · Armando Reis Tavares[5] · Marisa Domingos[1]

Received: 28 August 2025 / Accepted: 30 November 2025
© The Author(s) 2026

Abstract *Schinus terebinthifolia* (Raddi) is a tropical fast-growing broadleaf tree species in Brazil's Atlantic Forest, a threatened biodiversity hotspot. The species has socioeconomic importance, is used in forest restoration programs and urban greening. In urban environments, plants are exposed to several abiotic stressors such as atmospheric pollution. Tropospheric ozone (O_3) is one of the main secondary pollutants that affect plant growth and survival. Therefore, determining the critical levels (CL) of phytotoxic O_3 is essential. Ozone risk assessment for *S. terebinthifolia* is unknown. Forty-five *S. terebinthifolia* seedlings were cultivated in pots and submitted to five ozone treatments for three months in an O_3-free-air controlled facility. Ozone risk assessment was based on environmental data, measurements of stomatal O_3 uptake and seedling biomass. To find the best model for predicting O_3-induced biomass loss, we tested the accumulated ozone exposure over a threshold of 40 ppb (AOT40) and the phytotoxic ozone dose above a threshold 'y' (POD_y) using linear and 116 nonlinear statistical models. POD_{16} and POD_{15} when applied with the four-parameter nonlinear logarithmic model "Bragg4" provided the best fit for assessing O_3 risk based on total biomass and leaf biomass, respectively. The species had a 4% biomass loss at 2.56 mmol O_3 m^{-2} POD_{16} and in leaf biomass at 3.37 mmol O_3 m^{-2} POD_{15}. The results indicate that biomass accumulation was stimulated at low to moderate O_3 levels but reduced at higher levels. Overall, *S. terebinthifolia* demonstrated a high tolerance to tropospheric O_3.

Supplementary Information The online version contains supplementary material available at https://doi.org/10.1007/s11676-026-02033-y.

Project funding: This study was supported by Fundação de Amparo à Pesquisa do Estado de São Paulo (FAPESP – Process 2023/16524-0) and by EU—Next Generation EU Mission 4 "Education and Research"—Component 2: "From research to business"—Investment 3.1: "Fund for the realization of an integrated system of research and innovation infrastructures"—Project IR0000032—ITINERIS—Italian Integrated Environmental Research Infrastructures System—CUP B53C22002150006.

The online version is available at https://link.springer.com/

Corresponding editor: Tao Xu.

✉ Matheus Casarini Siqueira
matheus.casarini1@gmail.com

[1] Programa de Pós-Graduação em Biodiversidade Vegetal e Meio Ambiente (PPGBVMA), Environmental Research Institute (IPA), Av. Miguel Estefno, São Paulo 3687, 04301-012, Brazil

[2] Guarulhos University (UnG), Praça Tereza Cristina, 88, Guarulhos 07023-070, Brazil

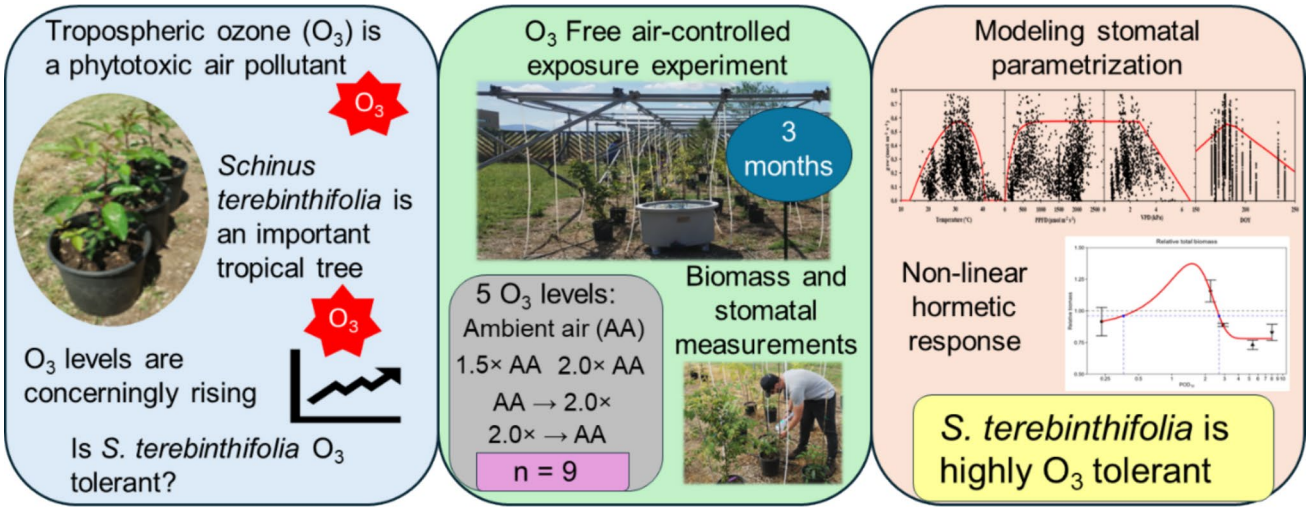
[3] Institute of Research On Terrestrial Ecosystems (IRET), National Research Council, Via Madonna del Piano 10, 50019 Sesto Fiorentino, Italy

[4] National Biodiversity Future Center (NBFC), 90133 Palermo, Italy

[5] Agronomic Institute (IAC), Av. Barão de Itapura, Jundiaí 1481, 13020-902, Brazil

Published online: 26 March 2026

Graphical abstract



Keywords Tropical environments · Ozone-stress · Tolerance · Hormetic biomass response · *Schinus terebinthifolia*

Introduction

Because of anthropogenic activities, emissions of primary air pollutants (CO_2, CH_4 and NO_x) have reached levels of concern in recent decades (Lamb et al. 2021). This has contributed to increasing levels of secondary air pollutants such as tropospheric ozone (O_3), which is formed in the presence of oxygen, primary pollutants (especially NO_x) and solar irradiation (Elshorbany et al. 2024). O_3 is a major pollutant that impacts air quality, climate, human health and ecosystems (Mills et al. 2018). Rising O_3 levels negatively impact the growth, development, and productivity of plant species, including crops and forests, representing a global environmental concern (Dewan and Lakhani 2022).

Multiple experimental approaches have been used to investigate the effects of O_3 on plants, with biomass production serving as a particularly relevant indicator of O_3-induced risk (Moura et al. 2018; Kaylor et al. 2023; Manzini et al. 2025). Studies using Free-Air Controlled Exposure (FACE) systems in open-air environments can provide reliable estimates of plant responses to O_3 under realistic environmental conditions (Paoletti et al. 2017; Hoshika et al. 2024).

The most commonly used exposure-based index for assessing O_3 risk to plant biomass production is the Accumulated Exposure Over Threshold of 40 ppb (AOT40), calculated based on tropospheric O_3 concentrations. However, since O_3 enters the leaf through the stomata, a flux-based index has proven to be more effective in predicting O_3-induced effects (Hoshika et al. 2024). The Phytotoxic Ozone Dose (POD_y, where "y" represents the O_3 flux threshold) accounts for actual O_3 uptake by plants, considering both climate conditions and plant physiological characteristics. As such, it provides a more specific and realistic dose–response relationship for accurate estimation of O_3 critical levels (CLs) (Mills et al. 2011).

In general, linear models are used to predict the impacts of O_3 exposure on biomass loss. However, recent studies have shown that plants subjected to O_3 stress may exhibit hormetic responses (Agathokleous et al. 2019a; Li et al. 2021), which are more evident in tolerant species (Hoshika et al. 2024). Hormesis (or hormetic response) is a dose–response characterized by a stimulatory or beneficial effect at low exposure to an environmental agent, followed by inhibitory or toxic effects at higher doses (Mattson 2008). In plants, the hormetic zone refers to a condition in which low stress levels enhance growth, biomass production, and/or active defense mechanisms. In contrast, higher doses can lead to adverse physiological effects and growth inhibition (Calabrese and Blain 2009). Since linear models do not adequately capture hormetic responses, testing nonlinear models is essential for accurately predicting plant response to O_3, particularly

for tolerant species which are often underrepresented in traditional dose–response studies based solely on linear modelling approaches (Agathokleous et al. 2019a).

Calculating O_3 flux, and consequently POD_y levels, requires species-specific parameterization to model stomatal O_3 uptake over time. This modeling is essential for determining critical levels associated with biomass loss. The ICP Vegetation Manual determines the CL based on a 4% biomass loss for tree species, particularly those in temperate climates (CLRTAP 2015). Although some parameterization of stomal conductance has been developed for subtropical tree species (Niu et al. 2016), studies involving tropical species are scarce. Only a few tropical species have been parameterized such as *Astronium graveolens* Jacq. (Cassimiro et al. 2016), *Eugenia uniflora* L. (da Silva Engela et al. 2021) and *Passiflora edulis* Sims (Fernandes et al. 2019). However, for these species, CLs for biomass loss have not been calculated, despite increasing O_3 concentrations in many South America cities (Seguel et al. 2024). Tropical climates favor a year-round O_3 formation (Moura et al. 2014), and this suggests that other tropical species from South America may also be at risk from elevated O_3, including *Schinus terebinthifolia* Raddi, commonly known as the Brazilian pepper tree. The species is native to Brazil's tropical Atlantic Forest, a highly threatened and important biodiversity hotspot (Marques and Grelle 2021). It has significant regional socioeconomic value (Lorenzi 2016), with recommendations for use in restoration and urban greening initiatives. Due to the species rapid growth and high tolerance to soil pollutants such as copper (Siqueira et al. 2021), iron (da Silva et al. 2024) and diesel fuel contamination (Bona et al. 2011), *S. terebinthifolia* shows attributes as an ideal plant model for stress tolerance studies.

Nature-based solutions (NBS) for mitigating the effects of climate change and air pollution in urban and peri-urban areas have become increasingly important (Hobbie and Grimm 2020). However, selecting suitable species for urban reforestation remains a complex task, particularly in cities where O_3 levels are rising (Nguyen et al. 2022). Urban reforestation must account for a wide range of plant traits, including morphological, physiological, and adaptive characteristics, highlighting species that provide high ecosystem services and exhibit tolerance to abiotic stressors (Miller et al. 2015). In this context, stomatal modelling and O_3 risk assessment for *S. terebinthifolia* are highly relevant for supporting public policies aimed at establishing limit concentrations of O_3. However, the response of this ecologically and economically important species to increasing O_3 levels is unknown, and thus defining ozone thresholds and plant-stress sensibilities can provide a scientific approach for tropical urban greening.

Therefore, we examined the stomatal conductance model for *S. terebinthifolia*. Linear and several nonlinear dose–response functions were compared to identify the most suitable for predicting the effects of increasing O_3 on *S. terebinthifolia* biomass using AOT40 and POD_y indices as exposure metrics. In addition, we determined the CL of O_3 capable of causing significant biomass loss. As *S. terebinthifolia* is tolerant to soil pollutants, it was hypothesized that it might also be ozone-tolerant and show a hormetic biomass response to increasing ozone concentrations.

Materials and methods

Ozone face fumigation set-up and experimental design

The experiment was carried out in a free-air O_3 exposure facility in Sesto Fiorentino, Italy (43°48′59″ N, 11°12′01″ E, 55 m a.s.l.), which allowed plant exposure to realistic environmental conditions. O_3 was generated from pure oxygen using an O_3 generator (TGOC13X, Triogen Ltd., Glasgow, UK), diluted with ambient air in a mixing tank and delivered through Teflon tubes suspended from a fixed grid above the plants (see Paoletti et al. 2017). Environmental parameters included air temperature (Temp, °C), relative humidity (RH, %) and solar radiation (SR, W m^{-2}), recorded hourly by a Watchdog station (Mod. 2000; Spectrum Technology, Inc., Aurora, IL, USA) positioned 2.5 m above ground level.

Seeds of *S. terebinthifolia* were obtained from a commercial nursery (Arbocenter, Brazil), sown in seedling trays in November 2023 and grown in a controlled environment (25 °C, Photosynthetic Photon Flux Density [PPFD]: 500 µmol m^{-2} s^{-1}) until spring 2024. The seedlings were subsequently transferred to the nursery and transplanted into 5 L pots containing 3.5 kg of natural soil. Ozone fumigation was carried out over three months during the summer of 2024 (day of year 161 to 259). Each pot received daily irrigation of 500 ± 50 mL d^{-1} via an automatic drip irrigation system, ensuring consistent soil water content throughout the experiment.

Plants were exposed for 90 d to three O_3 levels: ambient air (AA), 1.5 times the ambient O_3 concentration (1.5×), and twice the ambient O_3 concentration (2.0×). To establish intermediate O_3 exposures and thus create five treatments in total, plants from the AA and 2.0× groups were exchanged between plots midway through the experiment (45 d after the beginning on August 1st). These plants were subjected to 45 d under AA followed by 45 d under 2.0× (AA → 2.0×), and vice versa (2.0× → AA). These pots were randomly reallocated within the new treatment. The experimental design consisted of 45 *S. terebinthifolia* plants distributed across five treatments with nine plants per treatment arranged in replicated 5 × 5 m square plots (Fig. S1).

Biomass assessment

Biomass was determined at the beginning of the experiment (T_0) and at the end (B_{final}). At harvest, plants were separated into leaves, stems, and roots, oven-dried at 70 °C for 5 d until constant weight, then weighed using an analytical scale (Sartorius, Goettingen, Germany). Total plant biomass was calculated as the sum of the dry weights of leaves, stems, and roots.

Differences in total and leaf dry biomass among O_3 treatments were analyzed through one-way ANOVA, followed by Tukey's multiple comparison test ($p \leq 0.05$).

A control reference biomass (B_{ref}) was calculated for risk assessment, following Paoletti et al. (2017), assuming an average daily O_3 concentration of 20 ppb to represent the pre-industrial clean air condition (Tarasick et al. 2019). Relative biomass (B_{rel}) for both leaf and total biomass was then determined as the ratio: $B_{rel} = B_{final}/B_{ref}$.

Stomatal parametrization

Stomatal conductance to water vapor (*gsw*, mol m^{-2} s^{-1}), vapor pressure deficit (VPD, kPa) and leaf temperature (°C) as well as the environmental light (PPFD, µmol m^{-2} s^{-1}) were measured using a portable porometer (LI-600, Li-Cor Inc. Lincoln, NE, USA). These were used to parameterize the *gsw* model based on the multiplicative algorithm described by Jarvis (1976) and suggested by Mills et al. (2003) and Hayes et al. (2012) following the ICP-vegetation mapping manual (CLRTAP 2015):

$$gsw = g_{\max} \times f_{light} \times \max\left\{f_{\min}, \left(f_{temp} \times f_{VPD} \times f_{phen}\right)\right\} \quad (1)$$

where g_{max} (mmol O_3 m^{-2} s^{-1}) and f_{min} (fraction) are the maximum and minimum stomatal conductance (95th and 5th percentiles of all *gsw* data, respectively), following Bičárová et al. (2019) and Hoshika et al. (2020); the other functions indicate the response of stomata to environmental factors as photon flux density at the leaf surface (f_{light}), air temperature (f_{temp}), vapor pressure deficit (f_{VPD}) and phenology (f_{phen}). The accuracy of model estimation was assessed by performing a linear regression between the measured and estimated *gsw* values (Fig. S2), as described by Hoshika et al. (2012).

Measurements were taken twice per week on two fully expanded leaves at different positions on the main stem of each plant, resulting in 2048 measurements. These were designed to capture a wide range of VPD, temperature, and photosynthetic photon flux density (PPFD) conditions to evaluate *gsw* responses under variable environmental scenarios. The resulting parameterization was then used to calculate POD_y, based on the hourly stomatal O_3 flow (Hoshika et al. 2024).

Ozone indexes and critical levels (CLs) for risk assessment

The AOT40 index was calculated as the sum of the hourly O_3 concentrations exceeding 40 ppb during daylight hours (solar radiation ≥ 50 W m^{-2}), following the methodology established by the Convention on Long-range Transboundary Air Pollution (CLRTAP 2015).

POD_y was calculated by Eq. 2:

$$POD_y = \int \max\left(F_{st} - y, 0\right) \times dt \quad (2)$$

where "y" is a species-specific threshold of the hourly stomatal O_3 flux, and F_{st} (nmol m^{-2} s^{-1}) is calculated as in Eq. 3:

$$F_{st} = \frac{[O_3] \times g_s O_3 \times r_c}{\left(r_b + r_c\right)} \quad (3)$$

where $[O_3]$ is the hourly O_3 concentration (ppb); g_sO_3 (mol m^{-2} s^{-1}) is $gsw \times 0.663$, considering the diffusivity ratio between O_3 and water vapor (CLRTAP 2015); r_c is the leaf surface resistance calculated as $r_c = 1/g_sO_3 + 0.0164$ considering cuticular or external conductance (0.0164 mol m^{-2} s^{-1}, CLRTAP 2015) and r_b is the leaf boundary layer resistance calculated as $r_b = 1.3 \times 150 \times (L_d/\mu)^{0.5}$ where μ is the wind speed (m s^{-1}), L_d is the cross-wind leaf dimension (0.024 m, data obtained from de Souza Oliveira et al. 2019) and the factor 1.3 accounted for differences in diffusivity between heat and O_3 (CLRTAP 2015). Different POD_y detoxification thresholds were tested to identify the best POD_y index to predict O_3 effects on *S. terebinthifolia* total relative biomass.

Following the methodology of Hoshika et al. (2024), linear regression and 116 nonlinear statistical models were compared to identify the most suitable index for predicting biomass loss and leaf damage caused by O_3 toxicity. The analysis was conducted using the statistical software R, employing the packages "*drc*" (Ritz et al. 2015), "*modelr*" (Wickham 2023), "*aomisc*" (Onofri 2020), "*statforbiology*" (Onofri 2024) and "*automation*" (Ruiz 2023). Model selection was based on the following mathematical criteria: (1) lowest Akaike Information Criterion (AIC); (2) highest coefficient of determination (R^2); and (3) realistic biological responses (e.g., excluding models showing abrupt increases or decreases inconsistent with the plant's visual condition during the experiment).

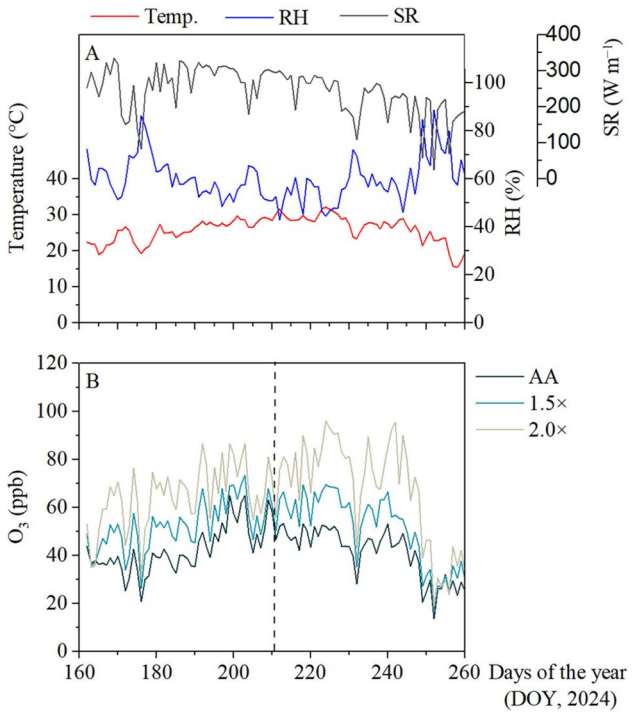


Fig. 1 **A** Daily means of solar radiation (SR), relative humidity (RH) and air temperature during the experiment. **B** Daily means of tropospheric O_3 exposure in ambient (AA), 1.5 times ambient (1.5×), and 2.0 times ambient (2.0×) air. Dashed vertical line represents the mid-term of the experiment and when part of the plants exposed to AA were switched to 2.0× (AA → 2.0×) and vice-versa (2.0× → AA)

Finally, the best-fitting model predictor was used to calculate the critical levels of tropospheric O_3 (CL) required to induce a 4% biomass loss (CLRTAP 2015). Graphs were generated using Microsoft Excel, GraphPad Prism or with "*ggplot2*" package in R. (Wickham 2016).

Results

Climate conditions and O_3 concentrations

During the experimental period, the mean daily solar radiation (SR) was 502.2 ± 249.9 W m^{-2}, the mean air relative humidity (RH) was 59.9% ± 19.4%, and the mean daily air temperature (T) was 25.8 ± 5.9 °C (Fig. 1A). SR gradually declined over the experimental period, while air temperature initially increased, reaching a peak on day 226 before decreasing in the latter half of the summer, while RH showed an opposite trend.

In treatments AA and 1.5×, daily mean O_3 levels increased during the first half of the experiment before declining toward the end. In contrast, the 2.0× treatment showed a slight increase beyond the midpoint before decreasing. The final O_3 mean hourly concentrations (ppb) were 39.9, 46.3, 53.0, 64.0 and 69.3 for AA, 2.0× → AA, 1.5×, AA → 2.0× and 2.0×, respectively.

Biomass

The final total dry biomass of *S. terebinthifolia* ($B_{final\text{-}T}$) increased in plants exposed to the 1.5× treatment, compared to all other treatments (Fig. 2A). In contrast, the final leaf dry biomass ($B_{final\text{-}L}$) was significantly reduced in plants exposed to treatments AA → 2.0× and 2.0×, relative to those exposed to 1.5× (Fig. 2B).

The calculated reference total biomass ($B_{ref\text{-}T}$) was 146.97 g (Fig. 3A), while the reference leaf biomass ($B_{ref\text{-}L}$) was 50.44 g (Fig. 3B).

The calculated values of relative leaf biomass ($B_{rel\text{-}L}$) were 0.89, 0.92, 1.08, 0.78 and 0.80. and those of relative total biomass ($B_{rel\text{-}T}$) were 0.92, 0.89, 1.16, 0.73 and 0.83 for AA, 2.0× → AA, 1.5×, AA → 2.0× and 2.0×, respectively.

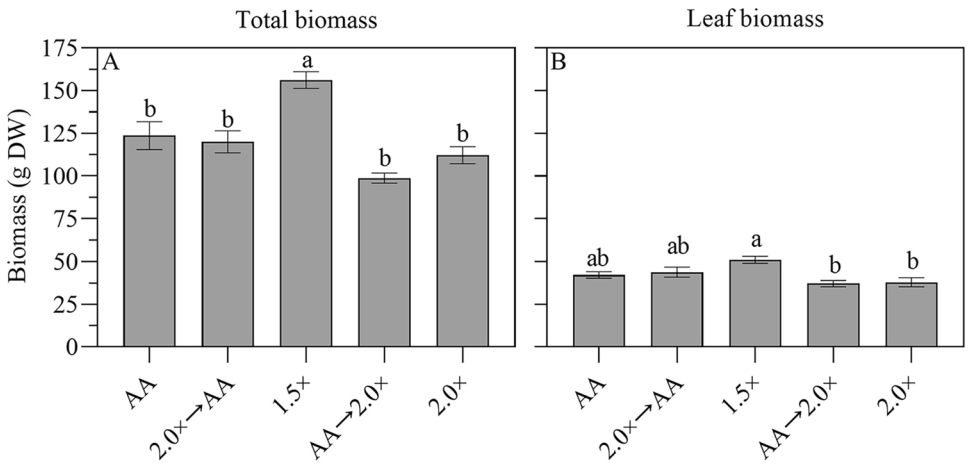


Fig. 2 **A** total and **B** leaf dry weight biomass (DW) of *S. terebinthifolia* plants after 90-d O_3 exposure in ambient air (AA), 1.5 times ambient air (1.5×), 2.0 times ambient air (2.0×), ambient to 2.0× after 45 d (AA → 2.0×) and 2.0× to ambient after 45 d (2.0× → AA) conditions. Distinct letters indicate significant differences according to one-way ANOVA followed by Tukey's test ($p \leq 0.05$). Bars denote standard error (n = 9)

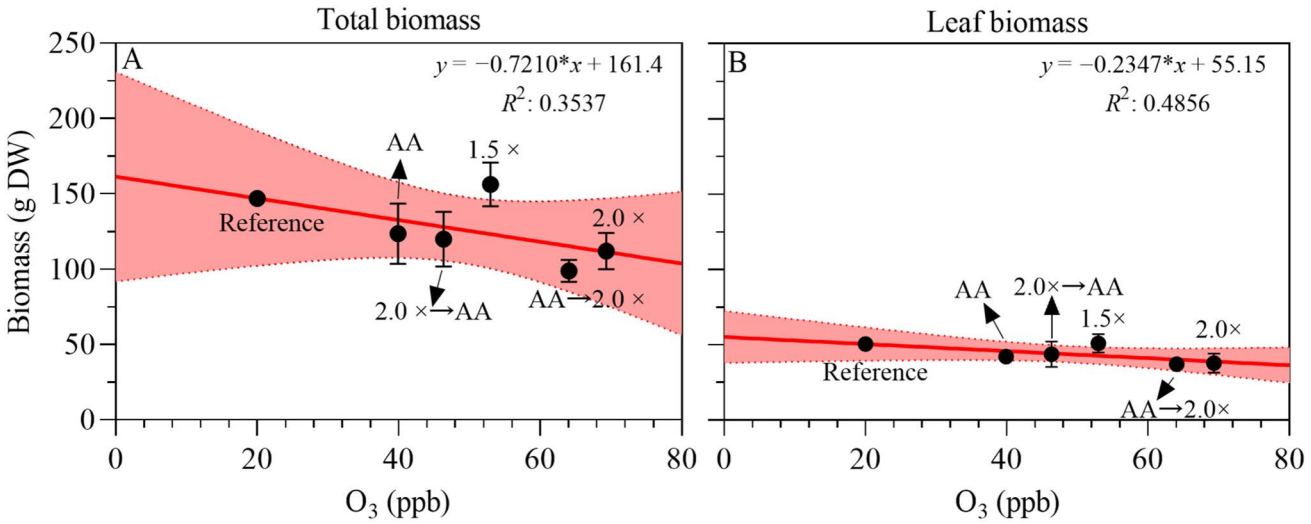


Fig. 3 Linear regressions of (**A**) total and (**B**) leaf biomass of *S. terebinthifolia* plants exposed to distinct O_3 treatments and calculated reference biomass. Bars denote standard errors ($n=9$). The red shaded areas represent the 95% confidence intervals. The regression equations and coefficient of determinations (R^2) are indicated in the upper right corner

Table 1 Stomatal conductance parameterization of *S. terebinthifolia* under natural conditions over the experimental period

Parameter		Unit	*S. terebinthifolia*
g_{max}		mol m^{-2} s^{-1}	0.575
f_{min}		Fraction	0.059
f_{temp}	T_{max}	℃	40.7
	T_{opt}	℃	31.3
	T_{min}	℃	13.3
f_{light}	*a*	Constant	0.0054
f_{VPD}	VPD_{max}	kPa	2.7
	VPD_{min}	kPa	6.5
f_{phen}	Start	d	161
	End	d	259
	f_{phen_a}	d	22
	f_{phen_b}	d	76

g_{max} is maximum conductance; f_{min} is the minimum stomatal conductance (fraction); f_{temp}, f_{light}, f_{VPD} and f_{phen} are the variation in g_{max} with temperature (T, °C), photosynthetic photon flux density (PPFD, µmol m^{-2} s^{-1}), vapor pressure deficit (VPD, kPa) and phenology (day of the year), respectively. T_{max}, T_{opt} and T_{min}, are the maximum, optimal, and minimum air temperature for stomatal opening. The constant a determines the shape of the exponential relationship for f_{light} function. VPD_{max} and VPD_{min} are the vapor pressure deficit for attaining maximum and minimum stomatal aperture. Start and End are the days of start and end of the experiment. f_{phen_a} and f_{phen_b} are the number of days for f_{phen} to reach its maximum and minimum, respectively

For both leaf and total biomass, *S. terebinthifolia* seedlings showed the highest relative biomass in the 1.5×treatment, while all other treatments resulted in lower values compared to the reference biomass estimated for pre-industrial conditions.

Stomatal parameterization and O_3 indexes (AOT40 and POD_{0-22})

The parameterization of *S. terebinthifolia* seedlings (Table 1) allowed for the modeling of stomatal conductance (Fig. 4), resulting in a maximum stomatal conductance (g_{max}) of 0.525 mol m^{-2} s^{-1}. The model identified an optimal temperature of 31.3 ℃, saturating light intensity (PPFD at *gsw* reached 90% g_{max}) of 1054 µmol m^{-2} s^{-1}, and a maximum vapor pressure deficit (VPD) of 2.7 kPa. Peak phenological activity occurred around the 180th day of the year.

AOT40 and POD_y values are shown in Table S1. POD_{22} was established as the upper limit because POD_y values became zero beyond this point for at least one treatment and thus are negligible.

Flux-based dose–response functions and critical levels detection

Tables S2 and S3 show the three best nonlinear and linear regression models for AOT40 and POD_y (0–22) as a function of $B_{rel\text{-}L}$ and $B_{rel\text{-}T}$. The regression ranking is defined according to the results of AIC and R^2 calculations for each index individually.

For both total and leaf relative biomass, the linear regression was not the most suitable predictor of *S. terebinthifolia* biomass across the tested indices, as it consistently exhibited high AIC values and low R^2. Among the 117 models tested (116 nonlinear plus the linear model), the linear model ranked between 33rd (in POD_{13} for $B_{rel\text{-}T}$) and 82nd (in POD_0 for $B_{rel\text{-}T}$).

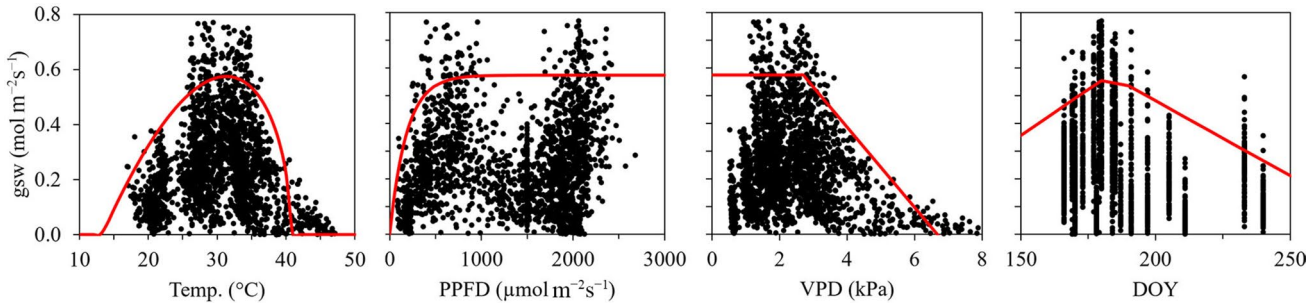


Fig. 4 Modeling of stomatal conductance (*gsw*, mol m^{-2} s^{-1}) of *S. terebinthifolia* as a function of temperature (℃), radiation (PPFD, µmol m^{-2} s^{-1}), vapor pressure deficit (VPD, kPa), and phenological activity (DOY–day of year). Black dots represent the measured stomatal conductance and the solid red line represents the calculated parametrization model for each environmental parameter

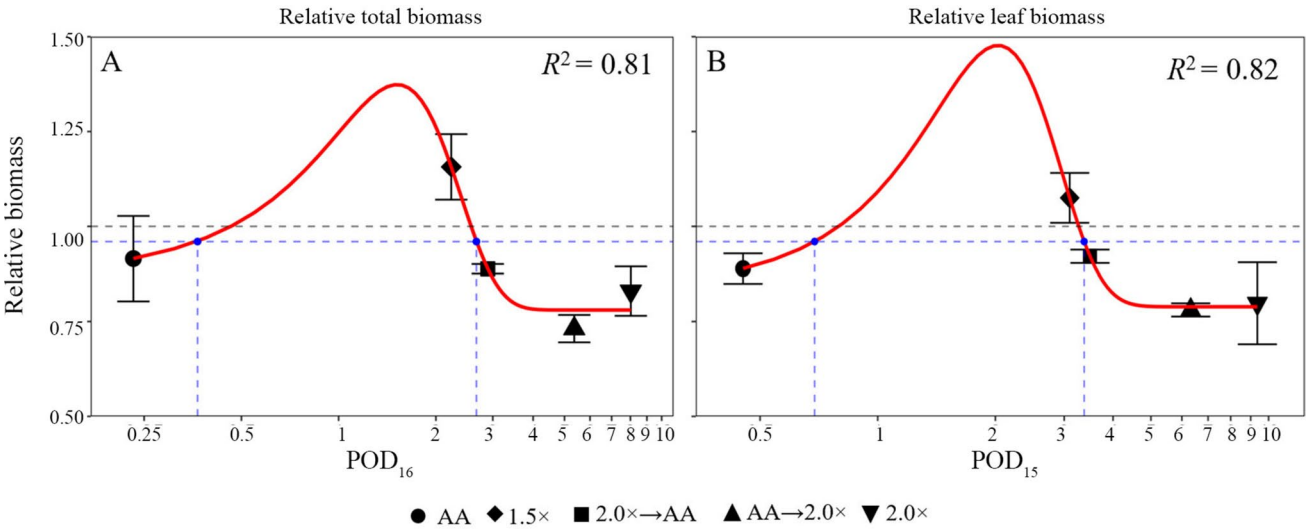


Fig. 5 Nonlinear Bragg.4 model applied as a predictor of *S. terebinthifolia* relative total biomass as a function of POD_{16} (**A**), and relative leaf biomass as a function of POD_{15}. The black dashed line represents the hypothetical relative biomass in the pre-industrial era ($B_{rel} = 1.00$). The blue dots and blue dashed line represent the O_3 critical levels to achieve 0.96 of relative biomass (4% biomass loss from the pre-industrial era). The black symbols represent *S. terebinthifolia* relative biomass (± SD) under each O_3 treatment, and the solid red line represents the calculated nonlinear model

In contrast, several nonlinear models demonstrated superior performance, with higher goodness-of-fit and more favorable AIC values. Among all combinations of models and indices, the best predictor of total biomass was the four-parameter logistic model "Bragg.4" (AIC = − 28.80, $R^2 = 0.81$) fitted to POD_{16} (Fig. 5A). For leaf biomass, the same nonlinear "Bragg.4" model was also the best fit (AIC = − 37.61, $R^2 = 0.82$) but based on POD_{15} (Fig. 5B).

Based on the best plausible model Bragg.4, the CLs to induce a 4% biomass loss were determined at 2.66 mmol O_3 m^{-2} POD_{16} for total biomass, and 3.37 mmol O_3 m^{-2} POD_{15} for leaf biomass.

Discussion

Although *S. terebinthifolia* is a native tropical species, the experiment was carried out in Italy, a non-tropical climate. However, the environmental variables throughout the summer showed moderate solar incidence (> 500 W m^{-2}), high relative humidity (> 50%) and mild temperatures (≈ 25 ºC), providing similar conditions to some Atlantic Forest regions in southern Brazil where *S. terebinthifolia* naturally occurs (Olmedo et al. 2023). *S. terebinthifolia* is also noteworthy for its remarkable ability to adapt to various types of climates and conditions (Santos et al. 2024). While the

environmental conditions proved to be adequate for *S. terebinthifolia* growth, factors such as various photoperiods and soil characteristics may influence the biomass response and constitutes a limitation of our study.

The mean hourly ozone concentration in ambient air (control) in Italy was approximately 40 ppb. In contrast, data from CETESB (2024) for the state of São Paulo (where the species is native and most of the remaining dense ombrophilous Atlantic Forest is located) in 2024, had a mean annual concentration of ≈ 82 ppb. This indicates that *S. terebinthifolia* is naturally exposed to even greater oxidative stress in its habitat than in our experiment. Consequently, the observed tolerance in our study possibly reflects an existing adaptation by the species to high ozone concentrations, supporting its potential use in urban settings in high-ozone regions like São Paulo. It is important to recognize that these high regional levels, monitored by CETESB (2024), also reflect the current reality of the Atlantic Forest biome which is fragmented and heavily affected by anthropogenic emissions from nearby metropolitan areas. Future dose–response studies within the remnants of the Atlantic Forest could further corroborate these findings.

The experimental conditions confirmed the effectiveness of the O_3-enrichment treatments in establishing distinct O_3 concentration levels, while maintaining a realistic environment for *S. terebinthifolia* growth under open-air conditions. As expected, the highest daily average O_3 levels were in the 2.0 × treatment and the lowest in ambient air (AA). Mid-experiment plant transfers between AA and 2.0 × treatments effectively created intermediate levels of O_3 uptake, demonstrating that this approach can effectively broaden the range of exposure scenarios without requiring additional O_3 generation systems. Moreover, this method provides a practical solution for exploring seasonal variations in plant responses to O_3 exposure.

The reductions in total and leaf biomass under elevated O_3 reflect O_3-induced physiological disruptions such as impaired photosynthetic efficiency (Xu et al. 2023), stomatal alterations (Hoshika et al. 2015), shifts in nitrogen and carbon allocation (Shang et al. 2019), and oxidative damage to cellular structures (Baier et al. 2005). However, there was an increase in total biomass under the 1.5 × treatment compared to the AA control, followed by a reduction, suggesting a hormetic response to mid-low O_3 exposure. In this case, negative effects on total plant biomass were evident only under high O_3, indicating a high capability of *S. terebinthifolia* to tolerate O_3-induced oxidative stress. Hoshika et al. (2024) suggested that moderate/tolerant species may exhibit broad response ranges and nonlinear patterns of biomass production under increasing O_3 exposure, which is consistent with the pattern observed in our study. In addition, after a 5 mmol O_3 m^{-2} dose, an almost flattened ozone-biomass response was exhibited. This indicates that the effect of O_3 on *S. terebinthifolia* biomass becomes negligible, reaching a saturation point and hormetic end zone (Erofeeva 2022), possibly due to limited stomatal O_3 uptake.

The POD_y index outperformed AOT40 in predicting both leaf and total biomass loss in *S. terebinthifolia*. Recent studies have demonstrated that POD_y provides greater accuracy than AOT40 in assessing O_3 effects on crop yield (Pleijel et al. 2022), biomass loss (Manzini et al. 2025) and for establishing CLs. However, to our knowledge, no study has tested several nonlinear regressions to assess biomass response to POD_y or AOT40. As a species-specific, flux-based index that accounts for plant physiology and stomatal behavior, POD_y yields more realistic estimates of O_3 impacts (Mills et al. 2011). In our study, the superior predictive performance of POD_y was confirmed, and its use is recommended for O_3 risk assessment and CLs calculation for this species. Importantly, the most effective POD_y thresholds for assessing *S. terebinthifolia* were those with higher "y" values, especially above 15 nmol O_3 m^{-2} s^{-1}. High "y" thresholds indicate substantial detoxification capacity by a plant species and may reflect an inherent tolerance to O_3 (Marzuoli et al. 2024). This suggests that *S. terebinthifolia* possess an effective defense system capable of mitigating oxidative stress from elevated O_3 uptake. Ongoing analyses of antioxidant activity and stress-related metabolic compounds may further clarify the physiological mechanisms underlying this apparent O_3 tolerance.

Regardless of the index used (AOT40 or POD_y), nonlinear models consistently outperformed linear regressions in predicting the effects of O_3 on *S. terebinthifolia* leaf and total biomass, as indicated by higher R^2 values and lower AIC scores. Therefore, our discussion is focused on the nonlinear models approach. The application of nonlinear models to assess O_3-induced effects on plant biomass has been previously reported in literature, with several studies highlighting their superior accuracy and greater biological realism compared to linear models (Agathokleous et al. 2019b; Conte et al. 2021). This confirms the accumulated scientific evidence indicating that plant responses to environmental stressors, including O_3, often follow nonlinear patterns (Hoshika et al. 2024). Nonlinear models are better suited to capture the complex dose–response dynamics that characterize plant physiological processes under variable environmental conditions.

However, the use of nonlinear models for O_3 risk assessment should be approached with caution. In our study, the four-parameter logistic model "Bragg.4" based on POD_{16} was selected as the most suitable model for predicting both leaf and total biomass loss of *S. terebinthifolia* under O_3 exposure. Mathematically, other models, specifically the "Five-parameter Cedergreen-Ritz-Streibig a" or "UCRS.5a" model on POD_{16} and the "Four-parameter Cedergreen-Ritz-Streibig a" or "UCRS.4a" model on POD_{19}, demonstrate even better performance in terms of lower AIC values and

higher R^2. However, despite their statistical superiority, these models were excluded due to their lack of biological plausibility. In particular, they produced abrupt shifts in biomass response across the O_3 gradient (Fig. S3 A) or failed to reflect a biological meaningful pattern in plant biomass production (Fig. S3 B). As highlighted by Tredennick et al. (2021), caution is warranted when applying nonlinear models as they can be prone to overfitting and may yield biological implausible interpretations. Our findings reinforce the importance of critically evaluating both the mathematical and biological validity of predictive models. When assessing O_3 risk, it is essential to prioritize models that not only perform well statistically but also reflect realistic biological responses to environmental stress.

Although we propose the use of nonlinear models to predict biomass response to O_3 exposure, linear regression was used to define the reference biomass in our study. The definition of reference biomass under ambient exposure conditions, such as those found in free-air O_3 enrichment (FACE) experiments, remains a subject of debate (Hoshika et al. 2024). Establishing a "zero dose" reference can potentially lead to overestimation of relative biomass, making the use of a constant reference value a more practical and widely accepted alternative (Paoletti et al. 2017). To address possible uncertainties associated with this estimated reference, we adopted the "modified Paoletti's approach" proposed by Hoshika et al. (2024), which incorporates the mean, upper, and lower bounds of the 95% confidence interval. Based on the "best fit" estimation (i.e., the intercept of the linear regression), *S. terebinthifolia* exhibited a broad range of biomass responses. This supports the hypothesis by Hoshika et al. (2024) that O_3-tolerant species tend to display a wider response range, possibly due to hormetic effects at low O_3 doses. We also used linear and nonlinear regressions without including the calculated reference value, relying only on the actual experimental data and avoiding biasing the modeling by starting from an arbitrary point (i.e., $B_{ref} = 1.0$), as done in previous ozone dose–response studies with experimental data (Hoshika et al. 2018; Manzini et al. 2025).

The critical level for *S. terebinthifolia* leaf and total biomass loss were determined based on POD_{16} and POD_{15}, respectively. In contrast, the CLRTAP (2015) convention recommends a threshold of 1 mmol m^{-2} s^{-1} (i.e., POD_1) for forest tree species. If POD_1 were applied to *S. terebinthifolia*, the estimated CL would be 39.13 mmol m^{-2} for leaf biomass and 38.98 mmol m^{-2} for total biomass (data not provided). However, a POD_1-based threshold assumes the species can only detoxify up to 1 nmol m^{-2} s^{-1} of absorbed O_3, with any additional uptake potentially causing physiological impairment. Our findings suggest otherwise. The species tolerance to O_3 and even stimulatory biomass effect observed at intermediate exposure levels (1.5×) indicate that *S. terebinthifolia* likely employs mechanisms beyond O_3 avoidance to maintain physiological functions and growth. Stomatal conductance data further support this, with high maximum stomatal conductance (g_{max}) of 0.525 mol m^{-2} s^{-1}, significantly exceeding values reported for other species, including *Cupressus sempervirens* L. (0.108 mol m^{-2} s^{-1}; Manzini et al. 2025), Mediterranean evergreen species *Quercus ilex* L. (0.250 mol m^{-2} s^{-1}), the Mediterranean species, *Quercus pubescens* Willd. (0.340 mol m^{-2} s^{-1}), deciduous broadleaf species such as *Quercus robur* L. (0.300 mol m^{-2} s^{-1}; Hoshika et al. 2018), *Alnus glutinosa* (L.) Gaertn. (0.300 mol m^{-2} s^{-1}), *Sorbus aucuparia* L. (0.240 mol m^{-2} s^{-1}), and herbaceous species like *Vaccinium myrtillus* L. (0.140 mol m^{-2} s^{-1}; Hoshika et al. 2020). The high stomatal conductance of *S. terebinthifolia* is evident when compared with other tropical species of the Atlantic Forest such as the moderately ozone-sensitive species *A. graveolens* Jacq. (0.152 mol m^{-2} s^{-1}; Cassimiro et al. 2016), the ozone-sensitive *E. uniflora* L. (0.082 mol m^{-2} s^{-1}; da Silva Engela et al. 2021) and the ozone-tolerant tropical liana species *P. edulis* Sims. (0.160 mol m^{-2} s^{-1}; Fernandes et al. 2019). This highlights that, even among species from the same biome and climate, the high stomatal conductivity of *S. terebinthifolia* is noteworthy.

Given this consistently high stomatal activity and POD_y (i.e., high O_3 flux threshold), it is unlikely that *S. terebinthifolia* mitigates O_3 stress through stomatal closure (i.e., an avoidance mechanism). Instead, the species possibly relies on active detoxication mechanisms, since *S. terebinthifolia* naturally synthesizes high levels of antioxidant compounds in leaves (Uliana et al. 2016; Oliveira et al. 2024), including ascorbic acid, glutathione and superoxide dismutase enzymes, key molecules known to mitigate O_3-induced oxidative stress (Siqueira et al. 2021). Therefore, it's possible that *S. terebinthifolia* relies on biochemical detoxification as a primary adaptive strategy to elevated O_3 stress, while maintaining sufficient stomatal opening for carbon uptake. Further studies focusing on antioxidant mechanism and physiological parameters might confirm this hypothesis.

Conclusion

This study presents the parametrization of the stomatal O_3 uptake model and O_3 risk assessment for *S. terebinthifolia*. The results support our hypothesis and suggest that *S. terebinthifolia* is highly tolerant to tropospheric O_3 stress. It is recommended to use the flux-based POD_y index as the most appropriate approach for assessing O_3 risk in this species, as it incorporates species-specific physiological responses. Critical levels were estimated at 2.66 mmol O_3 m^{-2} (POD_{16}) for total biomass and 3.37 mmol O_3 m^{-2} (POD_{15}) for leaf biomass, beyond which a 4% reduction in relative biomass is expected. Nonlinear models were more suitable

than traditional linear regression for capturing complex dose–response relationships, offering better fit and biological realism. Modest biomass production increase occurred under low to moderate O_3 exposure (1.5 ×), followed by biomass reduction at higher doses, suggesting consistence with hormesis effects. The species high stomatal conductance with high tolerance indicates that *S. terebinthifolia* tolerates O_3 not through ozone uptake avoidance but likely relying on detoxification mechanisms. Future analyses of antioxidant activity and related metabolic compounds may further clarify the underlying tolerance mechanisms. Given its resilience and adaptive traits, *S. terebinthifolia* shows potential for use in urban greening and reforestation programs, particularly in regions affected by elevated O_3 levels.

Acknowledgement We thank Leonardo Lazzara, Jacopo Manzini, Andrea Viviano, Elena Marra and Cesare Garosi for field support, and National Research Council of Italy (CNR)—Institute of Research on Terrestrial Ecosystems (IRET) for infrastructure and ozone FACE facility.

Funding The Article Processing Charge (APC) for the publication of this research was funded by the Coordenação de Aperfeiçoamento de Pessoal de Nível Superior - Brasil (CAPES) (ROR identifier: 00x0ma614).

Data availability All data is included in the paper and supplementary information.

Declarations

Conflict of interest The authors declare that they have no conflict of interest.

Open Access This article is licensed under a Creative Commons Attribution 4.0 International License, which permits use, sharing, adaptation, distribution and reproduction in any medium or format, as long as you give appropriate credit to the original author(s) and the source, provide a link to the Creative Commons licence, and indicate if changes were made. The images or other third party material in this article are included in the article's Creative Commons licence, unless indicated otherwise in a credit line to the material. If material is not included in the article's Creative Commons licence and your intended use is not permitted by statutory regulation or exceeds the permitted use, you will need to obtain permission directly from the copyright holder. To view a copy of this licence, visit http://creativecommons.org/licenses/by/4.0/.

References

Agathokleous E, Araminiene V, Belz RG, Calatayud V, De Marco A, Domingos M, Feng ZZ, Hoshika Y, Kitao M, Koike T, Paoletti E, Saitanis CJ, Sicard P, Calabrese EJ (2019a) A quantitative assessment of hormetic responses of plants to ozone. Environ Res 176:108527. https://doi.org/10.1016/j.envres.2019.108527

Agathokleous E, Belz RG, Calatayud V, De Marco A, Hoshika Y, Kitao M, Saitanis CJ, Sicard P, Paoletti E, Calabrese EJ (2019b) Predicting the effect of ozone on vegetation *via* linear non-threshold (LNT), threshold and hormetic dose-response models. Sci Total Environ 649:61–74. https://doi.org/10.1016/j.scitotenv.2018.08.264

Baier M, Kandlbinder A, Golldack D, Dietz KJ (2005) Oxidative stress and ozone: perception, signalling and response. Plant Cell Environ 28(8):1012–1020. https://doi.org/10.1111/j.1365-3040.2005.01326.x

Bičárová S, Sitková Z, Pavlendová H, Fleischer P, Fleischer P, Bytnerowicz A (2019) The role of environmental factors in ozone uptake of *Pinus mugo* Turra. Atmos Pollut Res 10(1):283–293. https://doi.org/10.1016/j.apr.2018.08.003

Bona C, da Silva MYB, de Rezende IM, de Oliveira Santos G, de Souza LA, Inckot RC (2011) Efeito do solo contaminado com óleo diesel na estrutura da raiz e da folha de plântulas de *Sebastiania commersoniana* (Euphorbiaceae) e *Schinus terebinthifolius* (Anacardiaceae). Acta Bot Bras 25(2):277–285. https://doi.org/10.1590/s0102-33062011000200003

Calabrese EJ, Blain RB (2009) Hormesis and plant biology. Environ Pollut 157(1):42–48. https://doi.org/10.1016/j.envpol.2008.07.028

Cassimiro JC, Moura BB, Alonso R, Meirelles ST, Moraes RM (2016) Ozone stomatal flux and O_3 concentration-based metrics for *Astronium graveolens* Jacq., a Brazilian native forest tree species. Environ Pollut 213:1007–1015. https://doi.org/10.1016/j.envpol.2016.01.005

CETESB (2024) Qualidade do ar no estado de São Paulo. CETESB, São Paulo. 140 p. (Série Relatórios). Available at: https://cetesb.sp.gov.br/ar/wp-content/uploads/sites/28/2025/06/Relatorio-de-Metodologia-para-Avaliacao-da-Qualidade-do-Ar.pdf

CLRTAP (2015) Mapping critical levels for vegetation. chapter III of manual on methodologies and criteria for modelling and mapping critical loads and levels and air pollution effects. risks and trends. UNECE convention on long-range transboundary air pollution; accessed on 11 Jul 2025 on Web at: www.icpmapping.org

Conte A, Otu-Larbi F, Alivernini A, Hoshika Y, Paoletti E, Ashworth K, Fares S (2021) Exploring new strategies for ozone-risk assessment: a dynamic-threshold case study. Environ Pollut 287:117620. https://doi.org/10.1016/j.envpol.2021.117620

da Silva PN, dos Reis CHG, Duarte VP, de Castro EM, de Pádua MP, Pereira FJ (2024) Toxicity of iron mining tailings and potential for revegetation using *Schinus terebinthifolia* raddi based on the emergence, growth, and anatomy of the species. Mining 4(3):719–732. https://doi.org/10.3390/mining4030040

da Silva Engela MRG, Furlan CM, Esposito MP, Fernandes FF, Carrari E, Domingos M, Paoletti E, Hoshika Y (2021) Metabolic and physiological alterations indicate that the tropical broadleaf tree *Eugenia uniflora* L. is sensitive to ozone. Sci Total Environ 769:145080. https://doi.org/10.1016/j.scitotenv.2021.145080

de Souza Oliveira V, Covre AM, Gouvea DS, Canal L, dos Santos KTH, Santos JSH, Santos GP, Pinheiro APB, Schmildt O, Posse RP, Czepak MP, Arantes SD, Alexandre RS, do Amaral JAT, da Vitória EL, Schmildt ER (2019) Determination of the leaflet area of *Schinus terebinthifolius* Raddi in function of linear dimensions. J Agric Sci 11(14):198. https://doi.org/10.5539/jas.v11n14p198

Dewan S, Lakhani A (2022) Tropospheric ozone and its natural precursors impacted by climatic changes in emission and dynamics. Front Environ Sci 10:1007942. https://doi.org/10.3389/fenvs.2022.1007942

Elshorbany Y, Ziemke JR, Strode S, Petetin H, Miyazaki K, De Smedt I, Pickering K, Seguel RJ, Worden H, Emmerichs T, Taraborrelli D, Cazorla M, Fadnavis S, Buchholz RR, Gaubert B, Rojas NY,

Nogueira T, Salameh T, Huang M (2024) Tropospheric ozone precursors: global and regional distributions, trends, and variability. Atmos Chem Phys 24(21):12225–12257. https://doi.org/10.5194/acp-24-12225-2024

Erofeeva EA (2022) Environmental hormesis of non-specific and specific adaptive mechanisms in plants. Sci Total Environ 804:150059. https://doi.org/10.1016/j.scitotenv.2021.150059

Fernandes FF, Esposito MP, da Silva Engela MRG, Cardoso-Gustavson P, Furlan CM, Hoshika Y, Carrari E, Magni G, Domingos M, Paoletti E (2019) The passion fruit *liana* (*Passiflora edulis* Sims, Passifloraceae) is tolerant to ozone. Sci Total Environ 656:1091–1101. https://doi.org/10.1016/j.scitotenv.2018.11.425

Hayes F, Wagg S, Mills G, Wilkinson S, Davies W (2012) Ozone effects in a drier climate: implications for stomatal fluxes of reduced stomatal sensitivity to soil drying in a typical grassland species. Glob Change Biol 18(3):948–959. https://doi.org/10.1111/j.1365-2486.2011.02613.x

Hobbie SE, Grimm NB (2020) Nature-based approaches to managing climate change impacts in cities. Philos Trans R Soc Lond B Biol Sci 375(1794):20190124. https://doi.org/10.1098/rstb.2019.0124

Hoshika Y, Watanabe M, Inada N, Koike T (2012) Modeling of stomatal conductance for estimating ozone uptake of *Fagus crenata* under experimentally enhanced free-air ozone exposure. Water Air Soil Pollut 223(7):3893–3901. https://doi.org/10.1007/s11270-012-1158-9

Hoshika Y, Watanabe M, Kitao M, Häberle KH, Grams TEE, Koike T, Matyssek R (2015) Ozone induces stomatal narrowing in European and Siebold's beeches: a comparison between two experiments of free-air ozone exposure. Environ Pollut 196:527–533. https://doi.org/10.1016/j.envpol.2014.07.034

Hoshika Y, Moura B, Paoletti E (2018) Ozone risk assessment in three oak species as affected by soil water availability. Environ Sci Pollut Res 25(9):8125–8136. https://doi.org/10.1007/s11356-017-9786-7

Hoshika Y, Carrari E, Mariotti B, Martini S, De Marco A, Sicard P, Paoletti E (2020) Flux-based ozone risk assessment for a plant injury index (PII) in three European cool-temperate deciduous tree species. Forests 11(1):82. https://doi.org/10.3390/f11010082

Hoshika Y, Agathokleous E, Moura BB, Paoletti E (2024) Ozone risk assessment with free-air controlled exposure (FACE) experiments: a critical revisit. Environ Res 255:119215. https://doi.org/10.1016/j.envres.2024.119215

Jarvis PG (1976) The interpretation of the variations in leaf water potential and stomatal conductance found in canopies in the field. Philos Trans R Soc Lond B Biol Sci 273(927):593–610. https://doi.org/10.1098/rstb.1976.0035

Kaylor SD, Snell Taylor SJ, Herrick JD (2023) Estimates of biomass reductions of ozone sensitive herbaceous plants in California. Sci Total Environ 878:163134. https://doi.org/10.1016/j.scitotenv.2023.163134

Lamb WF, Wiedmann T, Pongratz J, Andrew R, Crippa M, Olivier JGJ, Wiedenhofer D, Mattioli G, Al Khourdajie A, House J, Pachauri S, Figueroa M, Saheb Y, Slade R, Hubacek K, Sun LX, Ribeiro SK, Khennas R, de la Rue du Can S, Chapungu L, Davis SJ, Bashmakov I, Dai HC, Dhakal S, Tan XC, Geng Y, Gu BH, Minx J (2021) A review of trends and drivers of greenhouse gas emissions by sector from 1990–2018. Environ Res Lett 16(7):073005. https://doi.org/10.1088/1748-9326/abee4e

Li ZZ, Yang J, Shang B, Agathokleous E, Rubert-Nason KF, Xu YS, Feng ZZ (2021) Nonlinear responses of foliar phenylpropanoids to increasing O_3 exposure: ecological implications in a *Populus* model system. Sci Total Environ 767:144358. https://doi.org/10.1016/j.scitotenv.2020.144358

Lorenzi H (2016) Árvores brasileiras: manual de identificação e cultivo de plantas arbóreas nativas do Brasil, 7 ed. Plantarum, Nova Odessa

Manzini J, Hoshika Y, Danti R, Moura BB, Paoletti E, Della Rocca G (2025) Ozone risk assessment of common cypress (*Cupressus sempervirens* L.) clones and effects of *Seiridium cardinale* infection. J Environ Sci 151:441–453. https://doi.org/10.1016/j.jes.2024.03.026

Marques MCM, Grelle CEV (2021) The Atlantic forest: history, biodiversity, threats and opportunities of the mega-diverse forest. Springer International Publishing, Cham. https://doi.org/10.1007/978-3-030-55322-7

Marzuoli R, Faoro F, Picchi V, Gerosa GA (2024) Phytotoxic ozone dose–response relationships for durum wheat (*Triticum durum*, Desf.). Plants 13(5):573. https://doi.org/10.3390/plants13050573

Mattson MP (2008) Hormesis defined. Ageing Res Rev 7(1):1–7. https://doi.org/10.1016/j.arr.2007.08.007

Miller RW, Hauer RJ, Werner LP (2015) Urban forestry: planning and managing urban greenspaces. Waveland press.

Mills G, Pleijel H, Braun S, Büker P, Bermejo V, Calvo E, Danielsson H, Emberson L, Fernández IG, Grünhage L, Harmens H, Hayes F, Karlsson PE, Simpson D (2011) New stomatal flux-based critical levels for ozone effects on vegetation. Atmos Environ 45(28):5064–5068. https://doi.org/10.1016/j.atmosenv.2011.06.009

Mills G, Pleijel H, Malley CS, Sinha B, Cooper OR, Schultz MG, Neufeld HS, Simpson D, Sharps K, Feng ZZ, Gerosa G, Harmens H, Kobayashi K, Saxena P, Paoletti E, Sinha V, Xu XB (2018) Tropospheric Ozone Assessment Report: present-day tropospheric ozone distribution and trends relevant to vegetation. Elementa Sci Anthropocene 6:47. https://doi.org/10.1525/elementa.302

Mills G, Buker P, Hayes F, Emberson L, Werner W, Gimeno B, Pihl Karlsson G (2003) Developing ozone flux-effect models for white clover from the ICP Vegetation ambient air monitoring experiment. Swed Water Air Pollut Res Lab Publ IVL B: 128–139.

Moura BB, Alves ES, de Souza SR, Domingos M, Vollenweider P (2014) Ozone phytotoxic potential with regard to fragments of the Atlantic semi-deciduous forest downwind of Sao Paulo, Brazil. Environ Pollut 192:65–73. https://doi.org/10.1016/j.envpol.2014.05.014

Moura BB, Hoshika Y, Ribeiro RV, Paoletti E (2018) Exposure- and flux-based assessment of ozone risk to sugarcane plants. Atmos Environ 176:252–260. https://doi.org/10.1016/j.atmosenv.2017.12.039

Nguyen DH, Lin C, Vu CT, Cheruiyot NK, Nguyen MK, Le TH, Lukkhasorn W, Vo TDH, Bui XT (2022) Tropospheric ozone and NO_x: a review of worldwide variation and meteorological influences. Environ Technol Innov 28:102809. https://doi.org/10.1016/j.eti.2022.102809

Niu JF, Zhao P, Sun ZW, Zhu LW, Ni GY, Zeng XP, Zhang ZZ, Zhao XH, Zhao PQ, Gao JG, Hu YT, Zeng XM, Ouyang L (2016) Stomatal uptake of O_3 in a *Schima superba* plantation in subtropical China derived from sap flow measurements. Sci Total Environ 545:465–475. https://doi.org/10.1016/j.scitotenv.2015.12.122

Oliveira KC, Franciscato LMSS, Mendes SS, Barizon FMA, Gonçalves DD, Barbosa LN, Faria MGI, Valle JS, Casalvara RFA, Gonçalves JE, Gazim ZC, Ruiz SP (2024) Essential oil from the leaves, fruits and twigs of *Schinus terebinthifolius*: chemical composition, antioxidant and antibacterial potential. Molecules 29(2):469. https://doi.org/10.3390/molecules29020469

Olmedo GM, Raguse-Quadros M, Conrado GT, Oliveira JM (2023) Climatic signals on phenological patterns among tree species in a subtropical forest community. Neotrop Biol Conserv 18(3):191–208. https://doi.org/10.3897/neotropical.18.e103506

Onofri A (2020) The broken bridge between biologists and statisticians: a blog and R package, Statforbiology, IT. https://www.statforbiology.com

Onofri A (2024) statforbiology: Tools for Data Analyses in Biology. R package version 0.9.9. https://CRAN.R-project.org/package=statforbiology

Paoletti E, Materassi A, Fasano G, Hoshika Y, Carriero G, Silaghi D, Badea O (2017) A new-generation 3D ozone FACE (free air controlled exposure). Sci Total Environ 575:1407–1414. https://doi.org/10.1016/j.scitotenv.2016.09.217

Pleijel H, Danielsson H, Broberg MC (2022) Benefits of the Phytotoxic Ozone Dose (POD) index in dose-response functions for wheat yield loss. Atmos Environ 268:118797. https://doi.org/10.1016/j.atmosenv.2021.118797

Ritz C, Baty F, Streibig JC, Gerhard D (2015) Dose-response analysis using R. PLoS ONE 10(12):e0146021. https://doi.org/10.1371/journal.pone.0146021

Ruiz E (2023) Automation of statistical testing & non-linear modelling in R package version 0.1.0. https://github.com/leliotruiz/automation

Santos RS, Alencar JBR, Gallo R (2024) Modeling the current and projected distribution of Brazilian peppertree *Schinus terebinthifolia* Raddi (Anacardiaceae) in the Americas. Braz J Biol 84:e279769. https://doi.org/10.1590/1519-6984.279769

Seguel RJ, Castillo L, Opazo C, Rojas NY, Nogueira T, Cazorla M, Gavidia-Calderón M, Gallardo L, Garreaud R, Carrasco-Escaff T, Elshorbany Y (2024) Changes in South American surface ozone trends: exploring the influences of precursors and extreme events. Atmos Chem Phys 24(14):8225–8242. https://doi.org/10.5194/acp-24-8225-2024

Shang B, Yuan XY, Li P, Xu YS, Feng ZZ (2019) Effects of elevated ozone and water deficit on poplar saplings: changes in carbon and nitrogen stocks and their allocation to different organs. For Ecol Manag 441:89–98. https://doi.org/10.1016/j.foreco.2019.03.042

Siqueira MC, Kanashiro S, Domingos M, Rinaldi MCS, Tavares AR (2021) Physiological and biochemical changes in tree seedlings growing in urban forest soil contaminated with copper in São Paulo, Brazil. Plant Soil 464(1–2):149–163. https://doi.org/10.1007/s11104-021-04948-3

Tarasick D, Galbally IE, Cooper OR, Schultz MG, Ancellet G, Leblanc T, Wallington TJ, Ziemke J, Liu X, Steinbacher M, Staehelin J, Vigouroux C, Hannigan JW, García O, Foret G, Zanis P, Weatherhead E, Petropavlovskikh I, Worden H, Osman M, Liu J, Chang KL, Gaudel A, Lin MY, Granados-Muñoz M, Thompson AM, Oltmans SJ, Cuesta J, Dufour G, Thouret V, Hassler B, Trickl T, Neu JL (2019) Tropospheric Ozone Assessment Report: tropospheric ozone from 1877–2016, observed levels, trends and uncertainties. Elementa Sci Anthropocene 7:39. https://doi.org/10.1525/elementa.376

Tredennick AT, Hooker G, Ellner SP, Adler PB (2021) A practical guide to selecting models for exploration, inference, and prediction in ecology. Ecology 102(6):e03336. https://doi.org/10.1002/ecy.3336

Uliana MP, Fronza M, da Silva AG, Vargas TS, de Andrade TU, Scherer R (2016) Composition and biological activity of Brazilian rose pepper (*Schinus terebinthifolius* Raddi) leaves. Ind Crops Prod 83:235–240. https://doi.org/10.1016/j.indcrop.2015.11.077

Wickham H (2016) ggplot2: elegant graphics for data analysis. Springer-Verlag, New York

Wickham H (2023) modelr: Modelling Functions that Work with the Pipe. R package version 0.1.11. https://CRAN.R-project.org/package=modelr

Xu JX, Zhao H, Wang S, Zheng YF, Mai BR, Zhang X (2023) Assessment of photosynthesis and yield loss of winter wheat under ground-level ozone exposure. Environ Technol Innov 29:103013. https://doi.org/10.1016/j.eti.2023.103013

Publisher's Note Springer Nature remains neutral with regard to jurisdictional claims in published maps and institutional affiliations.